Characterization of Ti Kα radiation resulting from interaction of a highly intense laser pulse with a thin titanium foil

J. King[3], M. Key[1], C. Chen[1], R. Freeman[3,8], T. Phillips[1], K. Akli[3], M. Borghesi[5], M. Chen[1]
T. Cowan[4], S. Hatchett[1], J. Koch[1], K. Lancaster[2,7], A. MacKinnon[1], P. Norreys[2], P. Patel[1],
L. Romagnani[5], R. Snavely[1], R. Stephens[4], C. Stoeckl[6], R. Town[1], M. Zepf[5], B. Zhang[3]

[1] *Lawrence Livermore National Laboratory, Livermore, CA, USA*

[2] *Rutherford Appleton Laboratories, Chilton, Oxon, UK*

[3] *University of California-Davis, Davis, CA, USA*

[4] *General Atomics, San Diego, CA, USA*

[5] *The Queen's University of Belfast, Belfast, UK*

[6] *University of Rochester-LLE, Rochester, NY, USA*

[7] *The Blackett Laboratory, Imperial College, London, UK*

[8] *The Ohio State University, Columbus, OH, USA*

A demonstration has recently been made of ra-diography of implosions using a non-thermal Kα source generated with a high intensity picosecond laser pulse [1]. Absolute source brightness is important in assessing the potential of this diagnostic and we present here measurements and Monte-Carlo simulations of the Ti Kα back-lighter source.

Figure 1: Layout of the diagnostics used to characterize the Ti Kα back-lighter source.

The experiment was conducted at the Vulcan laser within the Rutherford Appleton Laboratory (RAL) in the UK. A set of radiographs were taken in which a back-lighting source was produced using a 1 ps CPA beam. The beam delivered an average of 49J, within an 800 μm by 400μm elliptical spot, onto a 25 μm thick Ti foil (Fig. 1).

The first of two instruments used to characterize the Kα source was a spherical Bragg crystal imager (Quartz 20$\bar{2}$3, 2d of 0.2749 nm, radius of curvature 38 cm, aperture 1.6 cm) used to spatially resolve the emission of the Kα back-lighter [2]. The crystal focused the 4.5 keV Kα photons with 10 μm spatial resolution and 7.9$\times$ magnification onto a cooled, 16-bit, 1"$\times$1", 1024$\times$1024 pixel CCD chip. The instrument observation angle was normal to the rear axis of the foil.

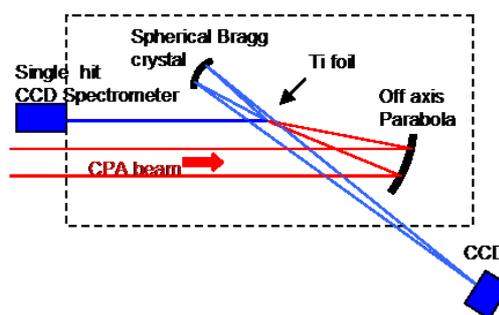The 2nd instrument was a single hit CCD spectrometer which was used to measure the ab-

solute Kα yield from the Ti target. The spectrometer consisted of a back-thinned CCD with 2048×2048 13.5 μm square pixels and a filter (100 or 150 μm Ti) that placed the chip in the single hit photon regime. The angle of observation was 41° from the rear surface normal of the Ti foil.

The single hit CCD spectrum was extracted as a pixel count histogram and the image thermal and Bremsstrahlung background were subtracted. The peak of this spectrum was then assigned the 4.5 keV energy of the Kα emission as illustrated in figure 2. The total number of Kα photons was deduced by integrating this Kα line. The absolute photon number was obtained by taking into account the transmission of the filters, the quantum efficiency of the CCD (0.6, from manufacturers data), the probability of a single hit (0.5), and the solid angle subtended by the analyzed area of the CCD.

Figure 2: Single hit CCD spectra of kα and Kβ

A 1024×1024 array of 16-bit numbers provided by the imaging CCD allowed us to obtain relative intensity maps of the Kα data. A uniform 450 count thermal background was subtracted and the images were integrated to find relative total Kα yields. These were then compared to the absolute total Kα yields, as determined by the spectrometer, to give a CCD calibration factor for absolute Kα brightness. Figure 3 shows a plot of this relative Kα yield against the absolute Kα yield.

The trend line for low yields indicates a linear relationship and gives an absolute calibration for the imager. At high yields, however, the data points fall significantly to the right of the trend line, effectively

Figure 3: Integrated Image vs. Kα yield. Low yield data points form a trend line whose slope gives an absolute calibration of the image brightness

separating the data into low and high yield sets. The average total number of Kα photons emitted in 4π steradians for these sets are 9.5×10^{11} and 3.3×10^{12}. With an average laser energy of 50J, the approximate Kα conversion efficiencies are then 1.4×10^{-5} for low yield and 4.9×10^{-5} for high yield. Differences in pre-plasma formation may be a possible explanation for the two
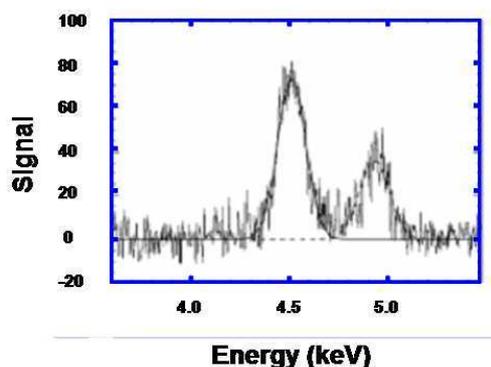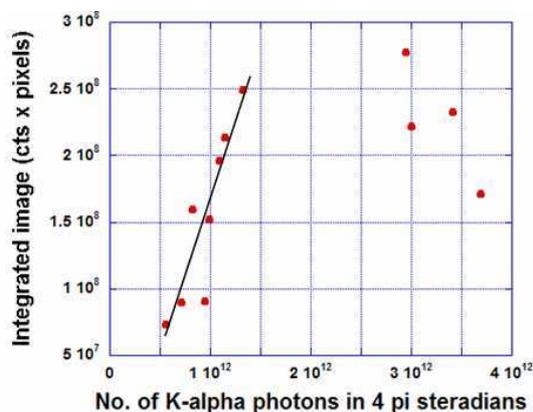
different behaviors. The ASE energy in a few nanoseconds before the pulse is about 1 J/cm^2. This is very close to the plasma formation threshold of a metal surface so that relatively small variations in the ASE can lead to larger variations in the preformed plasma. This can result in significant variations in the hot electron conversion efficiency and Kα production.

A Monte Carlo transport code employing ITS [3] was used to model the Kα emission from the Ti foil. Electrons were injected, with a 26° cone angle, into a circular irradiated area equal to the experimental area. A Boltzmann hot electron energy spectrum of average energy 57 keV was estimated from classical resonance absorption, at an average intensity I = 1.9×10^{16} W/cm^2, with the scaling $T_{hot} = 100 keV \times I_{17}^{1/3}$ as determined by Beg et al [4]. The Kα production was computed on the back surface of the foil and summed per steradian as a function of view angle. The results are plotted in figure 4. Also shown are the results of an isotropic injection of electrons. From the quotient of photons/sr as measured by the CCD spectrometer and the photons/sr/electron at an angle of 41° as given by the Monte Carlo model, the average numbers of 57 keV

Figure 4: Monte Carlo code results of Kα yield vs. angle from rear surface normal of a 25μm thick Ti foil. Also shown for comparison are the results of an isotropic injection of electrons.

electrons for the low and high yield data are 1.5×10^{14} and 5.2×10^{14}. This results in laser to electron energy conversion efficiencies of 3% and 10%, respectively. Again, this variation may be due to small variations in ASE which lead to larger variations in laser to electron energy conversion efficiencies.

Increased electron energy conversion efficiencie can lead to increased ionization induced shift of the Kα line [5]. An analytical model of energy deposition by supra-thermal electrons [6] provided energy density as a function of target depth for a given laser to electron energy conversion efficiency. This energy density was then related to the average ion charge state using the Los Alamos EOS library (Sesame) tables. Finally, a Multi-Configuration Dirac-Fock (MCDF) model [7, 8] was employed to relate the charge state to line shifts.

This line shifting can be sufficient to shift the line outside the bandwidth of the spherical crystal imager defined by the range of (Bragg) angles of incidence included in its aperture. We constructed a geometrical model giving the Kα collection efficiency of the crystal (relative
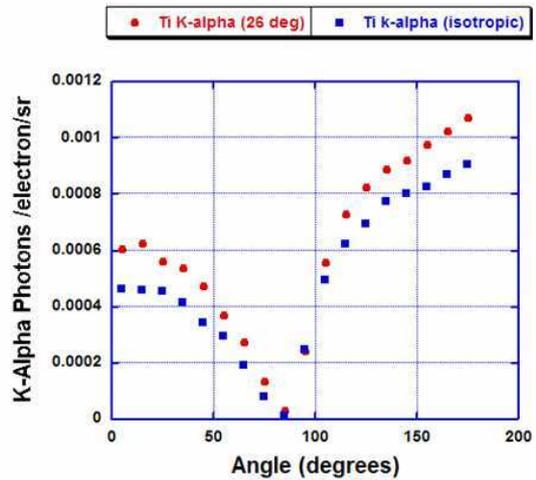
to cold Kα) as a function of energy shift and thus of target depth. The product of Kα yield, crystal collection efficiency and attenuation through the material was summed over all depths and divided by the total Kα yield to give the reduction of collected Kα as a result of ionization state shifting.

Figure 5 shows this relative collection efficiency vs. conversion efficiency of laser light to electrons for a hot electron temperature corresponding to an intensity of 1.9×10^{16} W/cm^2. The plot shows a reduction in collected Kα from ~100% to ~80% for the deduced increase in conversion efficiency from ~3% for low yield data to ~10% for high yield data. The discontinuity in the data in figure 3 therefore may be partially explained by a decrease in conversion efficiency associated with the pre-pulse ionization of the Ti target as discussed earlier.

Figure 5: As electron energy conversion efficiency is increased, a significant number of Kα photons are state shifted beyond the crystal bandwidth and the collection efficiency is reduced.

In conclusion, we have measured the absolute source brightness of a Ti Kα short pulse extended back-lighter, determined electron conversion efficiency through comparison of measured Kα with Monte Carlo modeling and finally, through comparison of the relative intensity of Bragg crystal Kα source images to the absolute intensity as recorded by a CCD spectrometer, noted changes in imaging crystal efficiency plausibly attributable to thermal line shifts of the Kα line.

References

[1] J. King et al, IFSA 2003, Edited by B.Hammel, D. Meyerhofer, J. Meyer-ter-vehn, and H. Azechi (Monterey, Ca. 2003) pp. 449-452

[2] J. Koch et al, Rev. Sci. Instrum. **7**, 2130 (2003)

[3] J. Halbleib and T. Mehlhorn, "ITS: The Integrated Tiger Series of Electron/Photon Monte Carlo Transport Codes" Sandia National Lab Report No. SAND84-0573, November, 1984

[4] F. Beg et al, Phys. Plasmas **4**, 447 (1997)

[5] E. Martinolli et al, Rev. Sci. Instrum. **75**, 2024 (2004)

[6] R. Harrach and R. Kidder, Phys. Rev. A **23**, 887, (1981)

[7] M. Chen, Phys. Rev. A **31**, 1449 (1985)

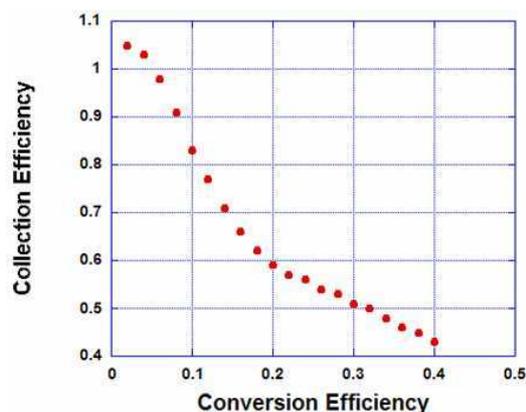[8] I. Grant et al, Comput. Phys. Commun. **21**, 207 (1980)